LETTER Communicated by Ad Aertsen

On Embedding Synfire Chains in a Balanced Network

Y. Aviel
aviel@cc.huji.ac.il
Interdisciplinary Center for Neural Computation, Hebrew University, Jerusalem, Israel

C. Mehring
Mehring@biologie.uni-freiburg.de
Neurobiology and Biophysics, Institute of Biology III, Albert-Ludwigs-University, Freiburg, Germany

M. Abeles
abeles@hbf.huji.ac.il
Interdisciplinary Center for Neural Computation, Hebrew University, Jerusalem, Israel

D. Horn
horn@post.tau.ac.il
School of Physics and Astronomy, Tel Aviv University, Tel Aviv, Israel

We investigate the formation of synfire waves in a balanced network of integrate-and-fire neurons. The synaptic connectivity of this network embodies synfire chains within a sparse random connectivity. This network can exhibit global oscillations but can also operate in an asynchronous activity mode. We analyze the correlations of two neurons in a pool as convenient indicators for the state of the network. We find, using different models, that these indicators depend on a scaling variable.

Beyond a critical point, strong correlations and large network oscillations are obtained. We looked for the conditions under which a synfire wave could be propagated on top of an otherwise asynchronous state of the network. This condition was found to be highly restrictive, requiring a large number of neurons for its implementation in our network. The results are based on analytic derivations and simulations.

1 Introduction

Synfire chains (SFCs) were introduced by Abeles (1991) as a model for solving a wide array of cognitive and computational tasks. They incorporate rate coding with specific synchronous activity and have been shown to be candidates for representing elementary cognitive functions (Bienenstock, 1995)

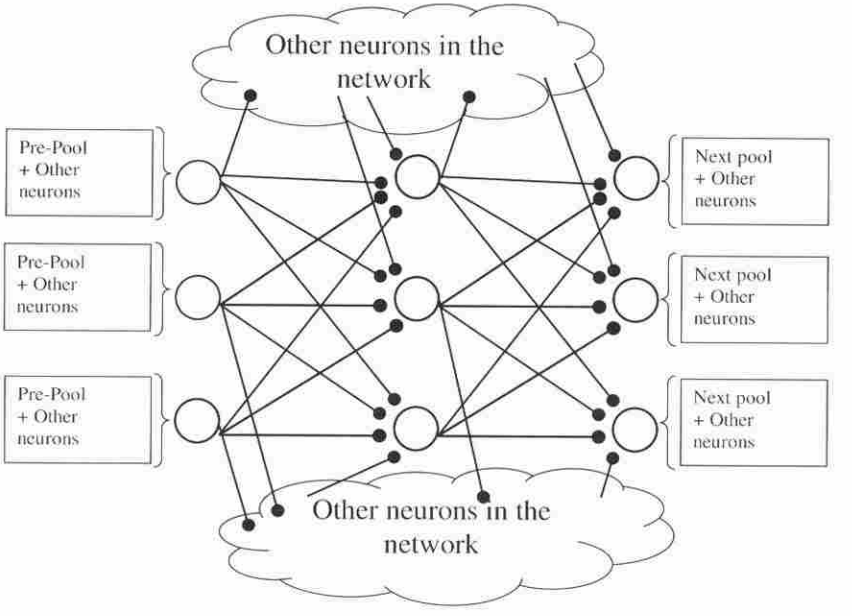

Figure 1: The connectivity of a synfire chain. The connection between three pools is shown. In the complete chain, each neuron in a pool receives inputs from all w neurons in the pre-pool ($w = 3$ in this figure). In addition, each neuron receives inputs from (and projects to) many other neurons in the network. Note that a neuron can participate in many pools.

such as binding (Hayun, 2002). An SFC dictates a well-defined connectivity pattern among neurons in the form of feedforward connections between pools of neurons. In a complete chain, all w neurons in a pool ("pre-pool") connect to all neurons in the successive pool, thus creating a chain of pools. Input connections as well as outputs are allowed, as shown in Figure 1.

If w, the number of neurons in a pool, is large enough, then a synchronized firing volley of most of the neurons in a pool, a *pulse packet*, may propagate along the chain (Diesmann, Gewaltig, & Aertsen, 1999). To avoid terminological confusion, these feedforward connectivity schemes are referred to henceforth as *chains* and the pulse packet propagating along a chain as a *synfire wave* (or simply a *wave*). A wave can propagate in a synchronized manner along a chain, or it can lose its synchrony, dissolving into the background activity. A wave is said to be stable if it reaches the end of the chain as a synchronized pulse packet.

We begin by focusing on a chain that is embedded in a large network, whose neurons produce some asynchronous low background activity. Each neuron in the chain receives occasional pulse packets from its pre-pool, as

well as some background activity. What are the effects of the background activity on the waves? Can waves travel along chains in a stable manner in the presence of background noise, or will they eventually dissolve into the background activity? Can the background noise cause spontaneous emergence of waves along chains? Diesmann et al. (1999) have shown that if the number of neurons in a pool is large enough and if the igniting pulse packet is synchronized and strong enough, the waves are stable in the presence of background noise.

Naturally, the next question is whether we can model a network that is capable of low spontaneous asynchronous activity with similar properties of a cortical tissue that is also capable of hosting stable synfire waves. In such a network, the effect of the background activity on the wave is important, but the effect of the chain on the asynchronous state of the network is also crucial.

In this letter, we investigate these issues by studying the correlations of two neurons that belong to the same pool. We show that the correlations allow us to distinguish between the different states of the network activity. High correlations occur when the system is in an oscillatory state, one where a synfire wave will be lost in the background of spontaneous activity. The challenge is to find the appropriate parameters such that stable waves exist in a background of asynchronous global activity and irregular spiking of individual neurons.

This problem arises from the existence of two constraints: on one hand, the system is required to maintain a stable asynchronous state, thus enabling rate coding, and on the other hand, we require the network to allow synchronous propagation of pulse packets—a kind of temporal code. Are these two modes mutually exclusive? As we shall see, it is possible to set up a network with physiological and anatomical realistic parameters that is capable of operating in both modes simultaneously.

In the context of the two-neuron problem, we use a simple, analytically amenable model that enables us to write an equation that describes the evolution of correlation along a chain. This equation is independent of the input firing rate and leads to the emergence of a new scaling variable. A more realistic integrate-and-fire neuronal model does show dependence on firing rates. Nevertheless, we find that the scaling variable still functions as a critical parameter. Moreover, the same holds not only for a pair of neurons, but also in the full network simulation. Our analysis, which is based on correlations, suffices for the discussion of the issues that we confront; hence, we do not delve into the evolution of firing rates (for the latter, see Tetzlaff, Geisel, & Diesmann, 2002).

Experimentally, neuron activity is typically characterized by steady low (2–5 Hz) firing rates, with irregular spiking (Abeles, 1991). To accommodate this observation with the known anatomical fact (Abeles, 1991) that there can be many inputs (around 20,000 excitatory and 2000 inhibitory synapses) to a neuron, it was suggested (Shadlen & Newsome, 1994; Gerstein & Man-

delbrot, 1964) that excitatory and inhibitory inputs cancel each other out, thus reducing the mean input to virtually zero. Thus, the firing of a neuron reflects fluctuations of the membrane potential that elicit occasional crossing of the threshold. Another solution (Softky & Koch, 1993) has been to argue that temporal correlation of the excitatory postsynaptic potentials (EPSPs) elicit neuronal firing. We consider a system that allows both solutions to coexist. First, the input is balanced, and second, waves of activity propagate by means of strong temporal correlation.

To create large fluctuations with a constant mean, we balance the excitatory input with an inhibitory input. A network is said to be balanced (van Vreeswijk & Sompolinsky, 1998) if each neuron in it receives equal amounts of excitation and inhibition. Its membrane potential will then fluctuate around some mean value and the firing process is noise driven, and therefore irregular. Balanced networks (BN) have been shown (Brunel, 2000) to mimic the in vivo firing statistics of cortical tissue, and it is therefore plausible that cortical neurons receive balanced input. BN has also been shown (van Vreeswijk & Sompolinsky, 1998) to have a stable asynchronous state, as well as appropriate rate coding properties, such as fast tracking of changes in external input rates.

Generally, BN assumes sparse and random connectivity. It is possible to embed SFCs in the excitatory-to-excitatory (E-E) connections of a BN, but this would violate the random connectivity assumption. Would this also disrupt the desired properties of a BN? As we show, there is a wide regime of parameters in which such lack of randomness has little effect.

2 The Model

Following Brunel (2000), we use an integrate-and-fire (IF) model, in which the ith neuron's membrane potential, $V_i(t)$, obeys the equation

$$\tau \frac{dV_i(t)}{dt} = -V_i(t) + RI_i(t), \tag{2.1}$$

where $I_i(t)$ is the synaptic current arriving at the soma and R is the membrane resistance. Spikes are modeled by delta functions; hence, the input is written as

$$RI_i(t) = \sum_j \sum_{t_j^f} J_{ij}\delta(t - t_j^f - D), \tag{2.2}$$

where the first sum is over different neurons, whereas the second sum represents their spikes arriving at times $t = t_j^f - D \cdot t_j^f$ is the emission time of the fth spike by neuron j, and D is a transmission delay, which we assume here to be the same for any pair of neurons. The sum is over all neurons that project their output to neuron i, both local and external afferents.

When $V_i(t)$ reaches the firing threshold θ, an action potential is emitted by neuron i, and after a refractory period τ_{rp}, during which the potential is insensitive to stimulation, the depolarization is reset to V_{reset}.

The following parameters were used in all simulations: the transmission delay $D = 1.5$ ms, the threshold $\theta = 20$ mV, the membrane time constant $\tau = 10$ ms, the refractory period $\tau_{rp} = 0.5$ ms, the resetting potential $V_{\text{reset}} = 0$ mV, and the membrane resistance $R = 40$ MΩ. The inhibitory and excitatory neurons have identical parameters.

We used the SYNOD simulation environment (Diesmann, Gewaltig, & Aertsen, 1995) for simulations with fewer than 10,000 neurons and a parallel version of SYNOD for simulation with more neurons. In the simulator, the Lapique (Tuckwell, 1988) model was used as an IF model with time steps of 0.1 ms.

Unless otherwise specified, we set the synaptic weights $J_{IE} = J_{EE} = J$, $J_{EI} = J_{II} = -gJ$ with $g = 5$ and $J = 0.14$ mV. The constant g is the relative strength of the inhibitory synapses, and J is the EPSP amplitude. Note that the synapses are weak, as $J \ll \theta$, and the total input to a neuron is approximately balanced.

When simulating a pair of neurons in a pool, the neurons receive local excitatory and inhibitory input from the network as well as external input from external excitatory sources that feed the entire network. For simplicity, we assume that the neurons have a single pre-pool. Thus, the neurons receive four types of input, three of which are local: K_I inhibitory synapses, w excitatory synapses that come from the previous pool, and $K - w$ excitatory synapses from other random connections in the network. The fourth type of input is represented by K excitatory synapses that convey external stimulation. Each of these inputs is modeled as an independent Poisson process with rates ν_I, ν_E, and ν_{ext} for the local inhibitory, local excitatory, and external excitatory synapses, respectively. In the simple model, which will be defined later, we refine the architecture further to include common inputs due to random connections. As a method for inducing correlations between spike trains, we use a "mother process": a Poisson process with rates ν/ρ^{in}, from which we copy spikes with probability ρ^{in}. The method is described in detail in Kuhn, Rotter, and Aertsen (in press). In order to measure the output correlation between two spike trains, we first binned the spike train into 1 ms bins (each spike is of width 0.1 ms) and then computed the zero-lag cross-correlation.

When simulating the entire network, we simulate all the N_E excitatory neurons, as well as the $N_I = N_E/4$ inhibitory neurons. A Poisson process with rate $\nu_{ext}K$ simulates the external input. ν_{ext} is in units of ν_{thre}, where $\nu_{thre} \equiv \frac{\theta}{JK\tau}$ is the minimal rate needed to emit a spike within τ milliseconds (on the average) in a neuron that does not get other inputs. In this article, we set $\nu_{ext} = 1.5\nu_{thre}$, which is equivalent to an external rate that ranges between 2 Hz and 21 Hz, depending on the value of K. The total input to a neuron is therefore nearly balanced. There is a small bias toward an excess of excitation, which controls the firing rates.

A sparse connectivity is required to both adhere as closely as possible to biological values and induce a source of randomness. Here we set the sparseness ε to be 0.1, that is, $K = \varepsilon N_E$, $K_I = \varepsilon N_I$. In addition to the external input (which are K excitatory afferents), each neuron in the network receives K excitatory and K_I inhibitory afferents, randomly sampled, from the excitatory and inhibitory population, respectively.

Wiring the network is performed as follows. In general, all the connections are chosen at random, except for the E-E connections, which are a superposition of chains. For wiring the E-E connections, each randomly chosen pool of w neurons is wired in an all-to-all fashion to the consecutive pool. We continue this process until the desired number of pools has been reached. We also ensure that a neuron will not receive more than K local connections. If a neuron does not receive K afferents and there are no more pools to be added, we randomly choose additional source neurons for it. At the end of the process, all the excitatory neurons have exactly K afferents, and there are chains hardwired into the connectivity matrix of the E-E connections.

The resulting connectivity is a mixture of random connectivity and chains. The number of pools is restricted by the number of excitatory synapses and is therefore less than $\frac{N_E K}{w^2} + 1$. In our simulation, we set the number of pools at 1000. If this was not possible due to the above limit, the simulation was not performed. A tighter bound on the number of pools is given by the capacity of the system, as discussed in section 6.

3 The Challenge

The foregoing enabled us to pursue the following scenario. We start with a BN that embodies chains in its connectivity matrix, as described in the previous section. In the absence of external ignition of a wave, we consider the state with global asynchronous activity to be the ground state of the system. External ignition of an SFC will perturb the system from its ground state, leading to wave propagation, masked by the overall activity. Once the ignited wave has reached the end of the chain, the system should return to its ground state.

Brunel (2000) has shown that BNs of IF neurons display four major stable states for different regimes of the external input rate, ν_{ext}, and the level of balance. The four states are all combinations of the two possible global (population-level) activities and the two possible neuronal firing patterns; the global activity can be either synchronous or asynchronous, whereas the neurons can fire in a regular or irregular fashion. Of special interest to us is the state that is characterized by asynchronous population activity and irregular neuronal firings. Following Brunel's terminology, this is the asynchronous-irregular (AI) state.

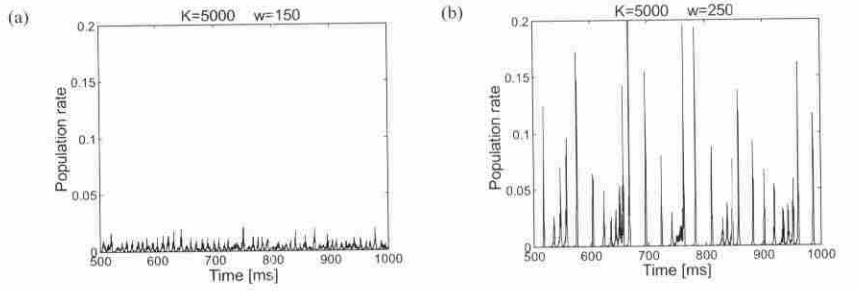

Figure 2: Population rate of a BN with embedded SFCs indicates a qualitative change in network behavior, as chain width increases. (a) With a chain of width $w = 150$, the network is in an AI state, characterized by low asynchronous population activity and very mild oscillations with small amplitudes. Average firing rate of the excitatory (inhibitory) neurons in this mode is 12.9 Hz (25.7 Hz). (b) Increasing the width to $w = 250$, a synchronous state appears, characterized by sporadic, abrupt synchronized bursts with large amplitudes. The average firing rate of the excitatory (inhibitory) neurons is 36 Hz (73 Hz). The population rate is the percentage of excitatory neurons that fired in 0.2 ms. The network parameters are $N_E = 50{,}000$, $K = 5000$, number of pools: 1000.

The network model described in section 2 is identical to Brunel's model except for the connectivity: in Brunel's model the connectivity is completely random, whereas we embody chains in the network. Another difference is in the dynamic parameters. Brunel varied ν_{ext} and g in order to obtain different states; here we vary only the chain width, keeping ν_{ext}, and g constant.

As shown in Figure 2a, a BN that embodies chains displays behavior similar to that of Brunel's AI state (Brunel, 2000). This suggests that a small departure from randomness does not refute the results obtained for random networks. Consequently, we use the AI state as the ground state of our system. We search through parameter space to find this regime in our model.

To allow stable propagation of a wave along a chain, we need large pools (Diesmann et al., 1999). However, when w is too large, as is the case in Figure 2b, the AI state loses its stability, with a transition similar to the phase transition that takes place in Brunel's model when moving from the AI state to the synchronous-irregular (SI) state. In the SI state, as in Figure 2b, the population activity is synchronous, and the neurons fire irregularly. (It should be noted, however, that the global oscillations in our case exhibit stronger irregularity than the one of Brunel's SI state. See Figure 8 there.) In the next section, we will see that the transition is due to high correlations between neurons with a relatively large common input. The challenge is to construct a network in which w is large enough to allow stable wave formation yet is not too large to destabilize the asynchronous state.

4 A Pair of Neurons

As hinted above, we suspect that in the case of large w, the embedded chains stimulate the emergence of correlated spike trains. To see this, consider a pool in a chain. The converging connections from the pre-pool to all the neurons in the pool induce an input that is common to all the neurons in that pool, possibly leading to correlations among these neurons' spike trains. This surplus of correlations underlies the instability of the asynchronous state in the full network.

We start by studying the effect of common inputs on a pair of neurons that belong to the same pool of an embedded chain. In particular, we are interested in the correlation coefficient between the spike trains of a pair of neurons in a pool, ρ^{out}. In Figure 3, we describe schematically a pair of neurons and their inputs. Being part of the same pool, they share a common input of at least w neurons from the previous pool (E_{cc}) and some other common input due to random connectivity (E_c and I_c). They also receive excitatory (E) and inhibitory (I) inputs that are independent for the two neurons. For simplicity, we assume that all inputs are uncorrelated, except for the w common input (E_{cc}) that have a pairwise correlation coefficient ρ^{in}.

We will define ρ^h to be the correlation coefficient between the two membrane potentials. The effect of the common input, w, on the correlation between two neurons, ρ^{out}, can be studied in two steps:

1. The effect of the common input on the correlation of the two membrane potentials: $\rho^h(w, K, \rho^{in})$.
2. The effect of the correlated membrane potentials on the correlation of the neurons' output: $\rho^{out}(\rho^h)$.

We start with a simplified neuronal model, in which a natural scaling of $w/\sqrt{K}$ emerges, and a transition in the level of correlations is found. We then proceed to an IAF model, where we find similar qualitative results.

4.1 A Simple Model. In the appendix, we define a semilinear model, the simple model, leading to an analytic expression of $\rho^h(w, K, \rho^{in})$:

$$\rho^h(\rho^{in}) = \frac{(1+g^2)\varepsilon K + w^2\rho^{in}}{(2+g^2)K + w^2\rho^{in}}. \tag{4.1}$$

Defining $q \equiv (2+g^2)$, and dividing the nominator and denominator by K yields

$$\rho^h = \frac{(q-1)\varepsilon + r^2\rho^{in}}{q + r^2\rho^{in}}, \tag{4.2}$$

where $r \equiv \frac{w}{\sqrt{K}}$, is the scaling variable of this system.

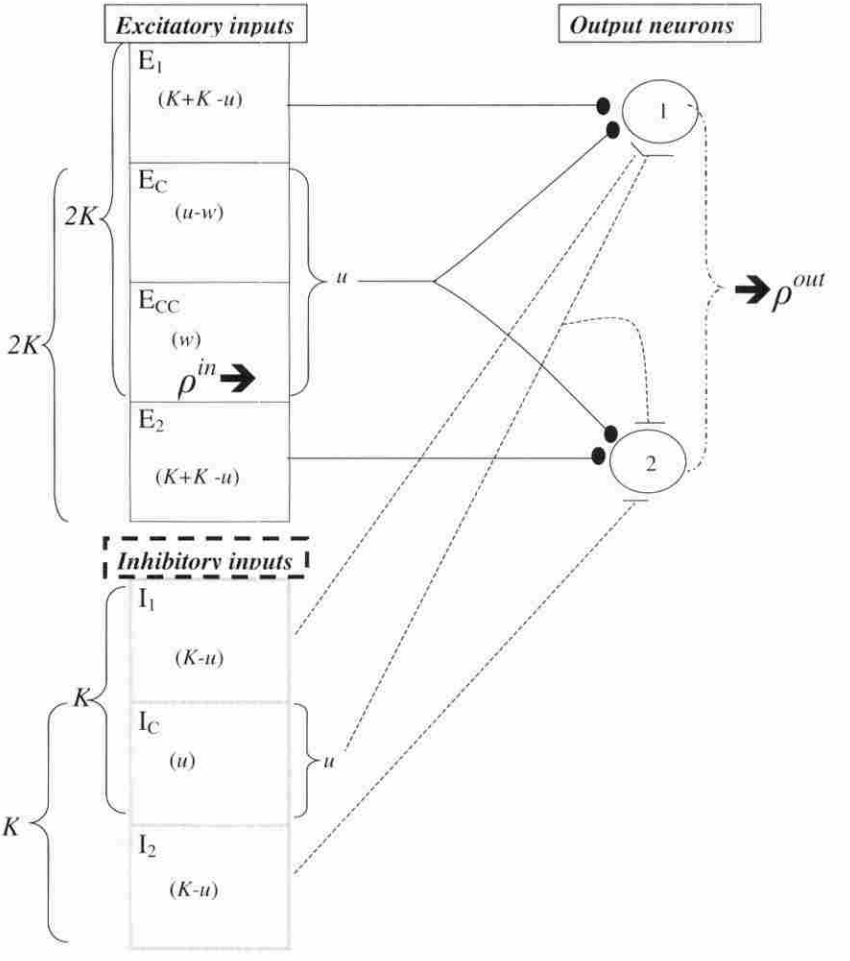

Figure 3: Two neurons of the same pool receive common input; the total input to each neuron is divided into five uncorrelated subfields: independent inhibitory and excitatory (E and I), common inhibitory and excitatory (E_c and I_c), and correlated common excitatory (E_{cc}) from the previous pool. Solid lines represent excitatory inputs and dashed lines inhibitory inputs. Expressions in parentheses denote the number of synapses that establish each type of input. The total number of excitatory inputs is $2K$, and the total number of inhibitory inputs that each neuron receives is K. Both neurons receive, on average, common input from u excitatory and u inhibitory neurons. The pairwise correlation assumed among inputs in E_{cc}, ρ^{in}, affects the correlation between the pair of output neurons, ρ^{out}.

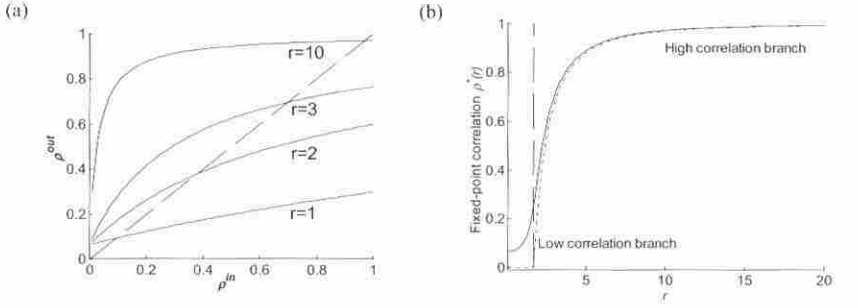

Figure 4: Transition in the simple model. (a) ρ^{out} as a function of ρ^{in} for different values of r: 1, 2, 3, and 10. The curves cross the diagonal (dashed line) exactly once, creating a globally stable fixed point. (b) The steady-state correlation (solid line, $\varepsilon = 0.1$) exhibits a transition from low to high correlation near the critical point, r_c (dashed line). In the limit $\varepsilon \to 0$, the transition becomes sharp (dash-dotted line). Parameters: $K = 10{,}000$, $g = 1$.

Note that ρ^h is not a function of the input or output rates in this model. Also note that for $r = 0$ and $\varepsilon > 0$, ρ^h is always positive. That means that even a pair of neurons with common input that is due to only the random connectivity tends to correlate. In a network where a pattern of connectivity as in Figure 3 is abundant, ρ^{out} of a pair of neurons is likely to be ρ^{in} for another pair of neurons. An example of such a network is one with chains hardwired into its connectivity matrix. In such cases, it is relevant to seek a fixed point of pairwise correlations, ρ^*, that obeys $\rho^{out} = \rho^{in} = \rho^*$. As argued in the appendix, under the constraint of equation A.5, $\rho^{out} = \rho^h$; thus, it is straightforward to look for such a fixed point.

In Figure 4a, the $\rho^{out}(\rho^{in})$ is plotted for several values of r. We note that $\rho^{out}(\rho^{in})$ crosses the diagonal with slope less than 1 exactly once, for all values of r, resulting in a globally stable fixed point: ρ^*. We calculate ρ^* from equation 4.2 by letting all ρ variables to be equal to ρ^* and taking the positive solution:

$$\rho^* = \frac{r^2 - q + \sqrt{(q - r^2)^2 + 4(q-1)\varepsilon r^2}}{2r^2}. \tag{4.3}$$

Two important observations follow from this equation. One is that the result is independent of the firing rate, which we assume is an artifact of the simplified model. The other is that the behavior of this equation is a function of the ratio r, and not of K and w separately. This implies that scaling w by $\sqrt{K}$ is the relevant scaling when considering correlation coefficients in this model.

Figure 4b displays ρ^* as a function of the scaling variable r. The curve displays a transition from low to high correlations near a critical value of

r, $r_c = \sqrt{q}$. Strictly speaking, the transition becomes sharp only in the limit $\varepsilon \to 0$. As can be observed in Figure 4b, in this limit, the stable fixed point is zero for r smaller than r_c, whereas above r_c it diverges rapidly.

4.2 An Integrate-and-Fire Model. When considering transmission of a highly correlated signal in an asynchronously active population, as we do in this study, two main variables should be examined: neuronal firing rates and correlations between neurons. Clearly, both variables depend on each other. Several studies have dealt with these variables. Tetzlaff, Buschermohle, Geisel, and Diesmann (2001) focused on the evolution of output rates as a function of input rates along a chain with noisy input but disregarded the issue of correlation. An integrative study, however, is currently being conducted by Tetzlaff et al. (2002). Salinas and Sejnowski (2000) studied the firing rates and their variability as a function of input correlation. The correlation in the input was a result of a common input or common oscillation in the input rates. Analytical results based on a random walk model with drift gave results that were qualitatively similar to a conductance-based IAF model. In addition, Feng and Brown (2000) discussed the impact of temporally correlated input on the output statistics of an IAF neuron. Stroeve and Gielen (2001) considered the correlation between a pair of neurons as a function of a correlated common input. They follow a logic similar to ours and compute $\rho^{out}(\rho^{in})$ for a conductance-based IF model; the resulting ρ^* was not derived. Here, we study the evolution of the output correlation as a function of the spatially correlated input in an IAF model.

The IF model is less amenable to analytic studies than the simple model. Hence, we turn to simulations in order to compute $\rho^{out}(r, \rho^{in}, \nu^{in})$. Note that we added the input firing rate ν^{in} as an additional parameter. This is due to the fact that input rates affect correlations of IF neurons (Salinas & Sejnowski, 2000; Stroeve & Gielen, 2001; Tetzlaff et al., 2001). Figure 5a shows $\rho^{out}(\rho^{in})$ for different w and for fixed values of K and ν_{in}. In contrast to the simple model, ρ^{out} can cross the diagonal more than once.

We look for the fixed-point correlations in the dynamic steady state of the system. Following the procedure used for the simple model, we extracted the intersection points of the curve with the diagonal $\rho^{out}(\rho^*) = \rho^*$. We also calculated the stability of these fixed points by measuring the slope at the point of intersection. The results are depicted in Figure 5b. If $|\frac{d\rho^*}{d\rho^{in}}| < 1$, the fixed point is stable (thick line); otherwise, it is unstable (thin dotted line).

Here, we define r_c to be the point where the saddle node bifurcation appears. Note that the details of the results of Figure 5 depend on the way correlations were introduced. Following the Poisson mother process, as explained in Kuhn et al. (in press), we introduced correlations well beyond the second order. Had we limited ourselves to currents with second-order correlations only, such as h_1 and h_2 of the appendix, the value of r_c would change considerably.

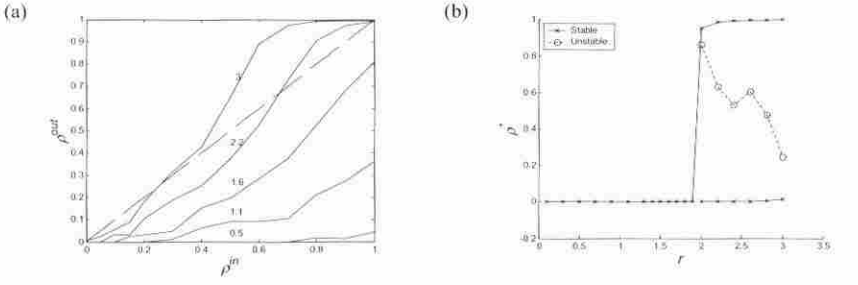

Figure 5: Transition in IAF neurons. (a) ρ^{out} as a function of ρ^{in} for different values of r (indicated above each curve). The crossings of the sigmoid curves and the diagonal (dashed line) yield the fixed-point correlations. (b) Fixed-point correlations as a function of r. Stable fixed points are indicated by a thick line and the unstable ones by a thin dotted line. Note that $\rho^* = 0$ is stable for any r in the range. Parameters: $K = 9000$, $\nu^{in} = 1.5^* \nu_{thre}$.

Unlike the simple model, we note that for small $r\rho^{in}$, $\rho^{out} \sim 0$. This insensitivity of the output correlation reflects the fact that the neurons' input is not completely balanced. Had the neurons' input been perfectly balanced, ρ^{out} would have been more sensitive to small input correlation. However, we chose the same neurons' parameters as in our simulations of the full network, so as to match the full network simulation better.

For $r > r_c$, the system is bistable. This is different from the simple model in Figure 4b, which had one global stable fixed point for any value of r. Note, however, that although this two-neuron system is bistable, this does not imply that a network of IF neurons will be bistable. Even if the network settles first in the lower (zero correlation) branch, transient spontaneous correlations may evolve, pushing the network into the basin of attraction of the upper branch. In fact, our network simulations described in the next section display either a low-correlation AI mode or a high-correlation synchronous mode of activity, depending on the parameters of the network. Moreover, we show in the next section that the critical behavior of the whole network displays scaling in the same variable r as predicted by the simple model.

5 The Full Network

The main lesson from our study of a pair of neurons is the existence of a rapid transition between low correlations to high correlations as function of the scaling variable $r = w/\sqrt{K}$. This type of behavior is also reflected in the simulations of IF networks. In our simulations, we use $K = N/10$. Running networks with different values of K (and N), we search for the transitions, as a function of w, of the networks from their AI mode to the global oscillatory mode. One possible measure is the coefficient of variance

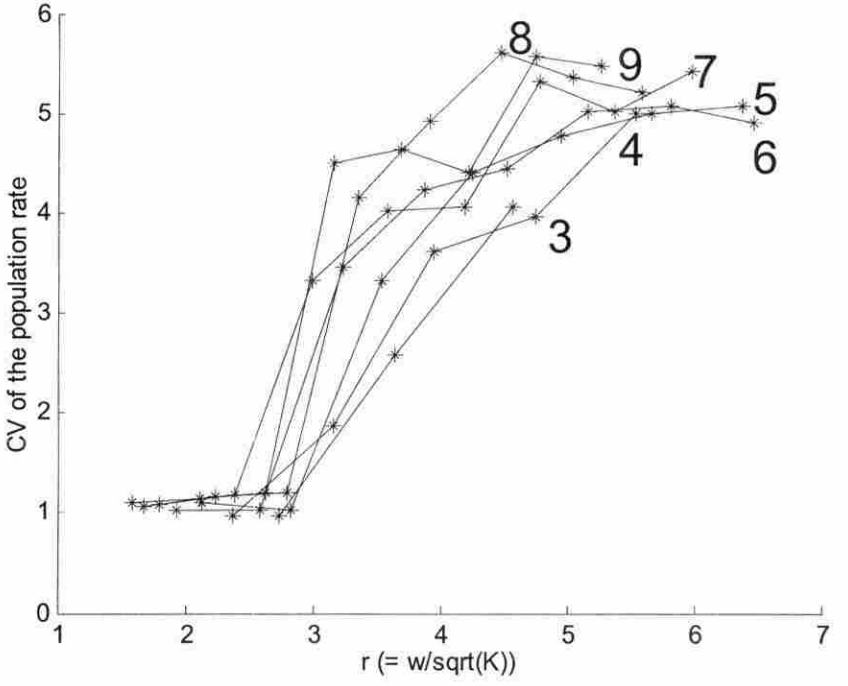

Figure 6: Scale invariance in the full network. The synchrony measure as a function of r for different network sizes. Digits inside the figure denote the size of K in thousands. w range from 150 to 500 in steps of 50. Population rate is defined as in Figure 2. Mean excitatory firing rate for $r \sim 2$ is 13 Hz (*SD* across the different population sizes 5). Mean excitatory firing rate for $r \sim 5$ is 41 Hz (*SD* 7).

(CV) of population rate defined as the standard deviation of population rate divided by the mean of population rate, shown in Figure 6. Plotting the results as function of the scaling variable r, we see that the different curves coincide; thus, this is a valid scaling relation for our problem. A sharp transition is observed around $r_c = 2.5$ in these networks.

Once we have gained some knowledge about the critical w, $w_c \equiv r_c\sqrt{K}$, above which strong correlations are inevitable, we can inquire whether w_c is large enough to enable a stable transmission of waves. Diesmann et al. (1999) pointed out that as w decreases, the basin of attraction of the stable pulse packets shrinks. Stated otherwise, there is a minimal w, $w_{\min}$, below which waves dissolve. Our challenge is meeting the contradicting requirements of small w, to avoid oscillations in the BN, and large w, to enable stable waves.

In short, we look for the range

$$w_{\min} < w < w_c, \tag{5.1}$$

where $w_{\min}$ depends on $\frac{\theta - v_{\text{reset}}}{J_{EE}}$. We conclude that K has to be large in order to find a range of w satisfying equation 5.1.

For our IF model parameters, we find $w_{\min} > 230$ and $r_c \approx 2.7$. We choose $r = 2.5$; therefore, $K > (\frac{230}{2.5})^2$, or simply $K = 9000$. Since in our architecture $K = \varepsilon N_E$, where $\varepsilon = 0.1$, we have to simulate $N_E = 90{,}000$ excitatory neurons and $N_I = 22{,}500$ inhibitory neurons before we are able to observe a synfire wave in a balanced network.

Figure 7 shows the results of the simulations that substantiate the theoretical analysis. A wave is ignited at $t = 1600$ ms. For Figure 7a, $w = 200 < w_{\min}$; it dissolves after activating four pools. In Figure 7b, $w_{\min} < w = 250 < w_c$. The wave propagates successfully, activating 50 pools (only the first 30 pools are shown). It should be noted, however, that due to the length of the chain, all wave ignitions lead to an oscillatory activity that eventually prevents the wave from reaching the end of the chain. For Figure 7c, $w = 300 > w_c$; global oscillations are obtained, drowning the synfire wave.

6 Summary

Many articles (Abeles, 1991; Diesmann et al., 1999; Hertz, 1999; Tetzlaff et al., 2002) discuss properties of a single chain with stationary noisy inputs. In this work, we take the discussion one step further by embedding the chain in a balanced network of IF neurons. By simulating the entire network, we take into account the mutual influence of the chain on the network, and vice versa.

By insisting on working with a full network, we discovered that the formation of synfire waves in a balanced network poses quite a challenge. In order to obey all constraints of equation 5.1, we need a network of $N = 90{,}000$ excitatory neurons or more. In other words, we conclude that large networks are needed in order to create the right conditions. Changing the details of the neuronal model could possibly reduce this high number of neurons. Reducing $w_{\min}$ to 100 (as is the case in Diesmann et al., 1999) cuts the lower bound of K to near 1300 rather than 9000, as in our case. As for the upper bound, it has been shown (Brunel & Hakim, 1999; Brunel, 2000) that the location of the transition from the asynchronous state to the synchronous state depends on the characteristics of synaptic processing (e.g., time constant, heterogeneity of time constant). Moreover, in recent simulations, we have seen that adding inhibitory neurons to synfire pools may change the conditions of our network.

Mehring, Hehl, Kubo, Diesmann, and Aertsen (in press) also studied a synfire chain embedded in a balanced network of locally connected IF neurons. They investigated the propagation of synchronous activity for dif-

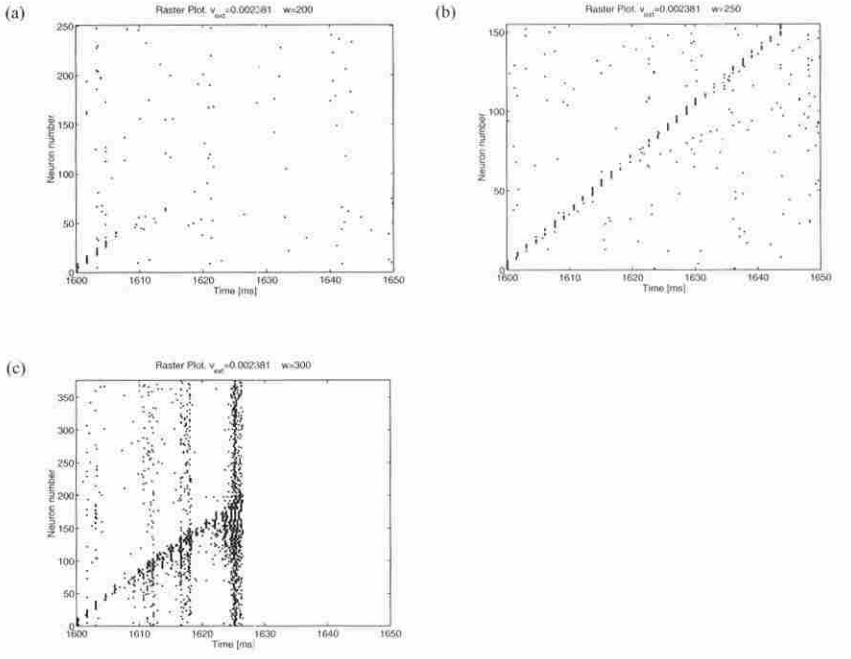

Figure 7: Three panels of raster plots. The neurons in the y-axis are ordered according to their participation in the pools. Only the first several pools are shown, where in each pool, every seventh neuron is presented. (a) Asynchronous activity. The wave ignited at $t = 1600$ dissolves ($w = 200 < w_{\min}$) (b) Asynchronous activity. The wave ignited at $t = 1600$ ms is stable. The first 30 pools are shown. ($w_{\min} < w = 250 < w_c$). (c) Synchronous activity, no meaningful wave obtained ($w_c < w = 300$). Parameters: $N_E = 90{,}000$. Mean excitatory/inhibitory firing rates of a, b, and c are 8/8, 4/13, and 26/24 Hz, respectively.

ferent spatial arrangements of a chain but did not analyze the instability of the AI state, as only short chains with 10 pools were considered. Tetzlaff et al. (2001, 2002) showed that for a chain with external Poissonian input, the transition from the asynchronous to synchronous regimes is well determined by a pure rate model. This seems to contradict our results. This apparent contradiction may be a result of the small r used by Tetzlaff et al. (2002). A closer look at their setup reveals that each neuron in their chain receives $K = 17{,}600$ excitatory inputs. Their chain width w is 200, hence their r is 1.41, which is small, probably smaller than their model's r_c. This explains the apparent contradiction. For small r values, correlation does not play a significant role, but rates apparently do. As mentioned before, firing rates and correlations affect each other in an intricate manner. Therefore, we have put emphasis on verifying that the qualitative scaling behavior of the

network, as depicted in Figure 6, holds for a range of external firing rates. There is always a critical r, but its value varies slightly as a function of the external rates, as can be expected from the IF model.

Previous studies within other models (Bienenstock, 1995; Hertz, 1999) have shown a critical dependence on the number of pools, a capacity limit analogous to that of stored memories in a feedback neural network. Here, by simulating a network of $N_E = 90{,}000$ and $w = 260$, we have found the capacity to be on the order of 2000 pools. Embedding a higher number of pools leads to spontaneous global oscillations. We conclude that all our previous results hold only below the capacity limit. If one exceeds the capacity limit, global oscillations will appear, regardless of the value of r.

There is current controversy between those who claim that neurons code information via their firing rate (Shadlen & Newsome, 1994) and those who believe that the information is conveyed in the exact timing of spikes (Softky & Koch, 1993). This debate engendered the concepts of balanced inputs (Shadlen & Newsome, 1994) and balanced networks (van Vreeswijk & Sompolinsky, 1998). Van Vreeswijk and Sompolinsky (1998) showed that BN has properties useful for rate coding performance. Here, we demonstrate that BN are capable of temporal coding as well. Furthermore, both codes can be applied simultaneously. Thus, the network may multiplex rate and temporal codes.

Appendix: The Simple Model

We define a semilinear neuronal model,

$$r_i(t) = [h_i(t)]_+, \tag{A.1}$$

where the function $[x]_+$ is x if $x > 0$ and zero otherwise. $h_i(t)$ is the local field, defined as a sum of K excitatory and K inhibitory synaptic inputs:

$$h_i(t) = \sum_{l=1}^{2K} J \cdot s_l(t) - \sum_{m=1}^{K} gJ \cdot s_m(t). \tag{A.2}$$

Here, J is the fixed synaptic weight, $s_l(t)$ is the presynaptic input at time t, and g controls the excess (or shortage) of excitation in the local field. The variables $s_l(t) > 0, l = 1 \cdots 3K$ represent the instantaneous firing rate of the presynaptic neuron. For clarity, we will discard the time notation of the s_l's. A semilinear model is a crude caricature of an IF neuron. Nevertheless, it enables the use of analytical tools, allowing for a better understanding of the phenomenon under inspection. Indeed, we find that a complex network of IF neurons exhibits behavior that is predicted by the current semilinear model.

A.1 Correlation Between Two Fields. Consider a pair of neurons in a pool, each having K external as well as K local excitatory synapses and K

inhibitory synapses, as depicted in Figure 3. As a result of random connectivity, some of these synapses share a source that is common to both neurons. The mean number of these inputs is taken to be $u - w$ for the excitatory synapses and u for the inhibitory synapses. Finally, there are w inputs that are common to both neurons, which come from the previous pool.

We divide the input field of a neuron into five subfields (see Figure 3):

- $2K - u$ synapses of external and local independent-excitatory input (E)
- $K - u$ synapses of independent-inhibitory input (I)
- $u - w$ synapses of common-excitatory input (E_c)
- u synapses of common-inhibitory input (I_c)
- w synapses of correlated-common-excitatory (E_{cc})

The I_c and E_c subfields represent common input due to the random connectivity. The E_{cc} subfield represents input that comes from the previous pool in the chain; thus, we also consider it as correlated input. To simplify the architecture without impairing its properties, we unite both the external and the local independent excitatory input into one subfield: E. The E and I subfields are different for the two output neurons; we denote the E subfield to the first and second neurons by E_1 and E_2, respectively. Similarly, I_1 and I_2 are the independent inhibitory subfields for the first and second neuron, respectively.

We assume that the s_i's are correlated stochastic variables that are characterized by their first two moments:

- $\langle s_i \rangle = \nu$
- $\mathrm{var}(s_i) = \sigma_s^2$
- $\langle s_i \cdot s_j \rangle = \rho^{in}\sigma_s^2 + \nu^2$, where ρ^{in} is the correlation coefficient.

Here, the angular brackets $\langle\ \rangle$ stand for an average over time or over different realizations of the s_i process. We assume no correlations among inputs that do not come from the previous pool; that is, ρ^{in} is 0 if i, j are not members of the same pool. This assumption may not be valid in a full network.

We calculate the membrane potential that is the result of incoming postsynaptic potentials in each of the five subfields. For example, the E_{cc} subfield is defined as $E_{cc} = \sum_{l \in E_{cc}}^{w} J \cdot s_l$, where J is the (single) synaptic weight. The synaptic of E_{cc} is as follows:

$$\mu_{E_{cc}} \equiv \langle E_{cc} \rangle = Jw\nu$$

$$\langle E_{cc}^2 \rangle = J^2 \left\langle \left(\sum_{l \in E_{cc}}^{w} s_l \right)^2 \right\rangle = J^2 w \langle s^2 \rangle + J^2 w(w-1)\langle s_i \cdot s_j \rangle$$

$$= J^2[w(\sigma_s^2 + \nu^2) + w(w-1)(\rho^{in}\sigma_s^2 + \nu^2)].$$

We assume w and K to be large; hence, we can apply the central limit theorem, leading to:

$$E_{cc} \sim N(\mu_{E_{cc}}, \sigma_{E_{cc}}), \text{ with } \mu_{E_{cc}} = Jwv$$
$$\text{and } \sigma_{E_{cc}} = J\sigma_s\sqrt{w(1+\rho_{in}(w-1))}.$$

A derivation similar to that of subfield E_{cc} leads to a normal approximation of the other subfields:

$$E_1 \sim N(\mu_{E_1}, \sigma_{E_1}), \text{ with } \mu_{E_1} = J(2K-u)v \text{ and } \sigma_{E_1} = J\sigma_s\sqrt{2K-u}$$
$$E_c \sim N(\mu_{E_c}, \sigma_{E_c}), \text{ with } \mu_{E_c} = J(u-w)v \text{ and } \sigma_{E_c} = J\sigma_s\sqrt{u-w}$$
$$I_1 \sim N(\mu_{I_1}, \sigma_{I_1}), \text{ with } \mu_{I_1} = -gJ(K-u)v \text{ and } \sigma_{I_1} = gJ\sigma_s\sqrt{K-u}$$
$$I_c \sim N(\mu_{I_c}, \sigma_{I_c}), \text{ with } \mu_{I_c} = -gJuv \text{ and } \sigma_{I_c} = gJ\sigma_s\sqrt{u}$$

Note that we assumed here that the inputs that do not come from the previous pool are uncorrelated, that is, $\langle s_i s_j \rangle = v^2$. Also note that $\mu_{E_1} = \mu_{E_2}$, $\mu_{I_1} = \mu_{I_2}$ and that $\sigma_{E_1} = \sigma_{E_2}$, $\sigma_{I_1} = \sigma_{I_2}$. Let h_1, the input field of the first neuron, be the sum of the five uncorrelated, normally distributed subfields of the first neuron: $h_1 = E_1 + E_c + E_{cc} + I_1 + I_c$. The statistics of h are as follows:

$$\mu_h \equiv \langle h \rangle = \langle E_1 \rangle + \langle E_c \rangle + \langle E_{cc} \rangle + \langle I_1 \rangle + \langle I_c \rangle = \mu_{E_1} + \mu_{E_c} + \mu_{E_{cc}} + \mu_{I_1} + \mu_{I_c}$$
$$\langle h^2 \rangle = \langle (E + E_c + E_{cc} + I + I_c)^2 \rangle = \sigma_{E_1}^2 + \sigma_{E_c}^2 + \sigma_{E_{cc}}^2 + \sigma_{I_1}^2 + \sigma_{I_c}^2 + \sigma_h^2.$$

Thus, $\sigma_h^2 = \sigma_{E_1}^2 + \sigma_{E_c}^2 + \sigma_{E_{cc}}^2 + \sigma_{I_1}^2 + \sigma_{I_c}^2 = J^2 + \sigma_s^2[(2+g^2)K + w(w-1)\rho^{in}]$. Similarly, we define $h_2 = E_2 + E_c + E_{cc} + I_2 + I_c$, where E_2 and I_2 are the respective subfields of the second neuron. Whereas $\langle h_2 \rangle = \langle h_1 \rangle$ and $\langle h_2^2 \rangle = \langle h_1^2 \rangle$, the covariance of the two fields depends on their common input:

$$\langle h_1 \cdot h_2 \rangle = \langle (E_1 + E_c + E_{cc} + I_1 + I_c)(E_2 + E_c + E_{cc} + I_2 + I_c) \rangle$$
$$= \sigma_{E_c}^2 + \sigma_{E_{cc}}^2 + \sigma_{I_c}^2 + (\mu_{E_1} + \mu_{E_c} + \mu_{E_{cc}} + \mu_{I_1} + \mu_{I_c})^2.$$

The correlation coefficient is:

$$\rho^h \equiv \frac{\langle h_1 \cdot h_2 \rangle - \mu_h^2}{\sigma_h^2} = \frac{\sigma_{E_c}^2 + \sigma_{E_{cc}}^2 + \sigma_{I_c}^2}{\sigma_{E_1}^2 + \sigma_{E_c}^2 + \sigma_{E_{cc}}^2 + \sigma_{I_1}^2 + \sigma_{I_c}^2}.$$

Finally, we get:

$$\rho^h = \frac{(1+g^2)u + w(w-1)\rho^{in}}{(2+g^2)K + w(w-1)\rho^{in}}. \tag{A.3}$$

The expected number of common inputs to pair of neurons in a pool, which is not from the pre-pool, is

$$(K-w)\frac{K-w}{N-w} = \varepsilon K \frac{(1-\frac{w}{K})^2}{1-\frac{w}{N}}.$$

Taking the leading order in K, we set

$$u = \varepsilon K. \tag{A.4}$$

Substituting equation A.4 in A.2 and using the approximation $w(w-1) \cong w^2$, we get equation 4.1.

A.2 Correlation Between Two Neurons. Clearly, the correlation between two neurons (ρ^{out}) is a function of the correlation between their fields (ρ^h). In general, however, this function is highly dependent on the neuronal model in use.

It is hard to derive an analytical expression of this dependency for nonlinear models. Therefore, we assume that the mean membrane potential, or the mean of the local field, is rarely below zero:

$$\mu_h > 2\sigma_h. \tag{A.5}$$

Thus $P[h_i(t) < 0] < 0.023$, which allows us to approximate equation A.1 with

$$r_i(t) \cong h_i(t). \tag{A.6}$$

This approximation allows us to equate the correlation between the neurons with the correlation between the fields, leading to

$$\rho^{out}(\rho^h) = \rho^h. \tag{A.7}$$

Acknowledgments

This work was supported in part by grants from GIF and BSF and Boehringer Ingelheim Fonds.

References

Abeles, M. (1991). *Corticonics*. Cambridge: Cambridge University Press.

Bienenstock, E. (1995). A model of the neocortex. *Network: Computation in Neural Systems, 6*, 179–224.

Brunel, N. (2000). Dynamics of sparsely connected networks of excitatory and inhibitory spiking neurons. *J. Comput. Neurosci., 8*(3), 183–208.

Brunel, N., & Hakim, V. (1999). Fast global oscillations in networks of integrate-and-fire neurons with low firing rates. *Neural Computation, 11*, 1621–1671.

Diesmann, M., Gewaltig, M. O., & Aertsen, A. (1995). *SYNOD: An environment for neural systems simulations*. Rehovot, Israel: Weizmann Institute of Science.

Diesmann, M., Gewaltig, M. O., & Aertsen, A. (1999). Stable propagation of synchronous spiking in cortical neural networks. *Nature, 402*(6761), 529–533.

Feng, J., & Brown, D. (2000). Impact of correlated inputs on the output of the integrate- and-fire model. *Neural Computation, 12*(3), 671–692.

Gerstein, G. L., & Mandelbrot, B. (1964). Random walk models for the spike activity of a single neuron. *Biophysical Journal, 4*, 41–68.

Hayun, G. (2002). *Modeling compositionality in biological neural networks by dynamic binding of synfire chains*. Unpublished doctoral dissertation, Hebrew University, Jerusalem.

Hertz, J. A. (1999). Modeling synfire networks. In O. Parodi (Ed.), *Neuronal information processing—From biological data to modelling and application*. London: Imperial College Press.

Kuhn, A., Rotter, S., & Aertsen, A. (in press). Correlated input spike trains and their effects on the response of the leaky integrate-and-fire neuron. *Neurocomputing*.

Mehring, C., Hehl, U., Kubo, M., Diesmann, M., & Aertsen, A. (in press). Activity dynamics and propagation of synchronous spiking in locally connected random networks. *Biol. Cyber.*

Salinas, E., & Sejnowski, T. J. (2000). Impact of correlated synaptic input on output firing rate and variability in simple neuronal models. *J. Neurosci., 20*(16), 6193–6209.

Shadlen, M. N., & Newsome, W. T. (1994). Noise, neural codes and cortical organization. *Curr. Opin. Neurobiol., 4*(4), 569–579.

Softky, W. R., & Koch, C. (1993). The highly irregular firing of cortical cells is inconsistent with temporal integration of random EPSPs. *J. Neurosci., 13*(1), 334–350.

Stroeve, S., & Gielen, S. (2001). Correlation between uncoupled conductance-based integrate-and-fire neurons due to common and synchronous presynaptic firing. *Neural Computation, 13*(9), 2005–2029.

Tetzlaff, T., Buschermohle, M., Geisel, T., & Diesmann, M. (2001). *The spread of rate and correlation in stationary cortical networks*. Paper presented at the Eleventh Computational Neuroscience Meeting, Monterey, CA.

Tetzlaff, T., Geisel, T., & Diesmann, M. (2002). The ground state of cortical feed-forward networks. *Neurocomputing, 44–46*, 673–678.

Tuckwell, H. C. (1988). *Introduction to theoretical neurobiology*. Cambridge: Cambridge University Press.

van Vreeswijk, C., & Sompolinsky, H. (1998). Chaotic balanced state in a model of cortical circuits. *Neural Computation, 10*(6), 1321–1371.

Received June 3, 2002; accepted December 5, 2002.